

# Uncertainty Quantification of Tiltrotor Whirl Flutter Aeroelastic Stability from Multibody Analysis

Federico Guerroni, Alessandro Cocco, Andrea Zanoni\*, Pierangelo Masarati.

Politecnico di Milano, Milano - Italy \*

andrea.zanoni@polimi.it

## Abstract

Tiltrotor aircraft maximum horizontal flight speed is limited by whirl flutter. Current research efforts focus on one side on experimentally investigating on the stability margins through specialized wind tunnel test-beds, and on the other side on developing efficient numerical tools, to both guide the development and gain information from experimental efforts. In this work, the development of TiPa, a software package providing a customizable interface to the general-purpose multibody dynamics solver MBDyn to provide a parametric tiltrotor model generation and investigation tool is presented. The tool is combined with DAKOTA, a state of the art Uncertainty Quantification (UQ) tool to form a complete aeroelastic stochastic analysis package. Two strategies for the parametric model generation are presented. One is based on the definition of complete MBDyn tiltrotor models while the other one relies on the generation of two different subsystems to be assembled through a substructuring approach. Some promising early results and assessment are presented, together with the expected future research direction.

## 1 INTRODUCTION

Tiltrotors, due to their capability of vertical takeoff and landing and high-speed forward flight, received increasing attention in the last several decades. Their design is mature enough to make possible their entrance in the civil air transport market [1].

Tiltrotor design is a challenging engineering task to the multipurpose missions to be accomplished by this aircraft. As a representative example, the case of whirl flutter is discussed in this work. Whirl flutter, a specific type of aeroelastic flutter instability [2, 3], is a phenomenon that is known to affect both turboprop and tiltrotor aircraft [4].

When a rotor mounted on a flexible structure rotates, the normal vibration modes associated to the elastic behaviour of the supporting structure are merged into precession modes. A point on the rotor axis of rotation draws circular paths about its initial position, changing the way each rotor blade perceive the incoming air speeds and generating a new set of aerodynamic loads. When this phenomenon is triggered, such forces can lead to the divergence of the system response and to the whirl flutter instability [5].

Nowadays, the understanding of the phenomenon in tiltrotor aircraft is still limited. Since many factors, for instance geometrical design, materials, actuators dynamics, can contribute to its occurrence, getting an accurate prediction of the aircraft aeroelastic behaviour can be very complicated.

The research group of the authors has been involved in numerous research activities focused on the multibody aeroelastic modeling of tiltrotors [6]. Parametric multibody

modeling of the vehicle has been used as the primary tool in order to study the sensitivities that each design parameter play on this phenomena.

Within this research frame, a MATLAB tool aimed at the automatic generation of arbitrary tiltrotor multibody parametric models, currently in development by the authors, is presented. The tool has been called TiPa (Tiltrotor Parametric model generator). It generates a model suitable to be simulated with MBDyn (<http://www.mbdyn.org/>), a general purpose multibody software with well established aeroelastic capabilities.

Furthermore, TiPa is able to manage the interaction between MBDyn and DAKOTA (<https://dakota.sandia.gov/>), an open source software under GNU LGPL licence widely used in the research community to perform uncertainty quantification and optimization [7]. The aim is to develop a comprehensive tool for uncertainty quantification in rotorcraft analysis, focusing in particular on stability analysis of tiltrotor configurations.

The present work describes the design approach followed in the development of TiPa, describes its capabilities and presents some early results related to the WRATS [6] tiltrotor flutter analysis.

## 2 TIPa

The development of a parametric tiltrotor whirl flutter prediction tool is meant to satisfy specific investigation requirements. Whirl flutter is an aeroelastic phenomenon affected by a large number of factors. The need to understand how each design feature influences a specific system aeroelastic behaviour is crucial in gaining further insights on the origin of instability phenomenon.

The easy adaptability of TiPa models allow this type of investigation. First, it is designed to provide a semiautomatic model generator for an arbitrary user defined proprotor configuration. The process is based on three input cards that store information about the system features and the required simulation properties. The software is designed to handle different amounts of input data in order to match the specific level of knowledge about the model configuration. Such information is used by TiPa to prepare input files for MBDyn. It can, furthermore, directly manage the MBDyn simulation, in order to automatically complete the aeroelastic assessment of the current design. Finally, TiPa also acts as a postprocessor for the response variables provided by MBDyn analysis. Such tasks are designed to make TiPa simulation flexible in order to be coupled with the external Uncertainty Quantification software DAKOTA.

## 2.1 Parametric Modeling

The software requires the definition of a series of input variables to be manipulated by TiPa internal schemes in order to generate the desired geometries. These input parameters are accessible through textual (MATLAB format) input cards:

1. the control card contains the parameters designed to control the current simulation, like
  - which assembly components to generate and analyze;
  - the model structure;
  - the air data for the aeroelastic assessment;
  - the postprocessing operations;
2. the wing card stores the user defined information required to model the wing subsystem;
3. the rotor card contains information about the rotor geometrical, aerodynamic and structural definition.

As evidenced by the different input cards, TiPa handles the model generation dividing the tiltrotor entire assembly into two parts (or subsystems): the wing and the rotor/pylon. This allows to write the rotor equations of motion in the rotating frame, and apply the multiblade coordinates (MBC) transformation to the subsystem matrices.

The wing subsystem definition and analysis is depicted graphically in Fig. 1. Please note that in the figure, the direct interaction between the user and the solver elements is represented with dashed lines, while all the other actions are represented by continuous lines. The TiPa preprocessor module is responsible for transforming the user defined data regarding the wing geometrical and structural parameters, contained in the wing card and regarding the requested analysis type and conditions, contained in the control card, into information compatible with MBDyn and printing the MBDyn input file.

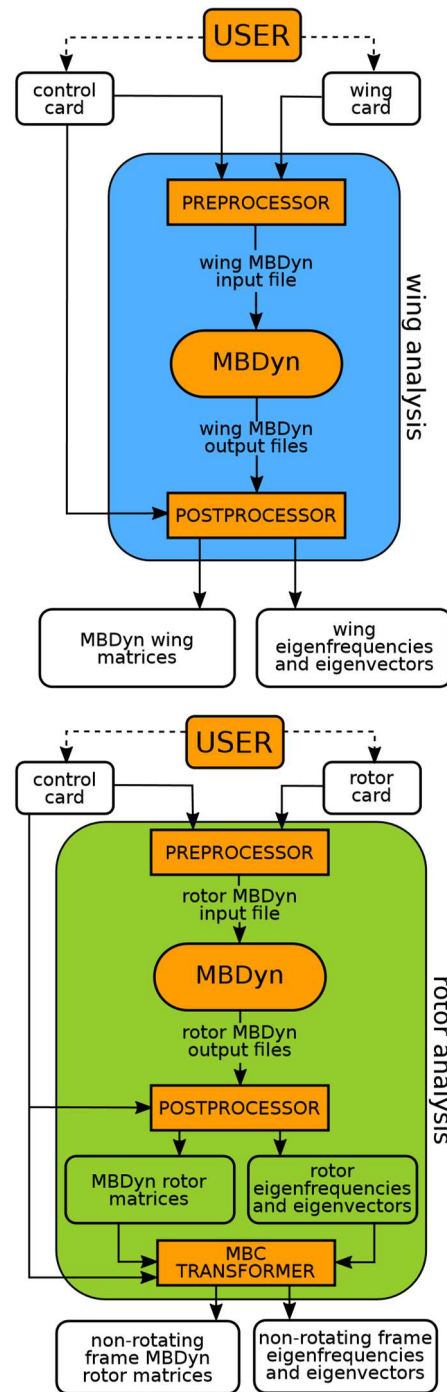


Figure 1: TiPa wing and rotor submodels analyses flowcharts.

The input file is then provided to MBDyn to execute the user defined requested simulation. TiPa makes extensive use of MBDyn eigenanalysis [8], since its output files store information about the modelled multibody system equations. The extraction of the wing subsystem matrices and modal parameters is devolved to the TiPa postprocessor module.

A similar procedure is followed to generate the rotor submodel (Cf. Fig. 1). As an optional post-processing step, the user can enable the MBC transformer module, that applies multiblade coordinate transformation (MBC) to the system matrices. As results, the MBDyn rotor subsystem is now described through the non-rotating frames DOFs. The user can select to directly combine the two subsystems and obtain a complete model of

the tiltrotor wing-pylon-rotor structure. In this case, both the wing and the rotor submodels are written in the non-rotating frame (Cf. Figs. 2,6).

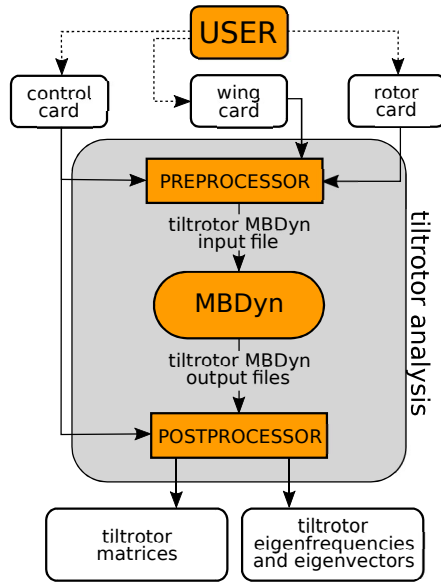


Figure 2: TiPa conventional tiltrotor model generation and analysis.

## 2.2 Substructuring

The MBDyn wing and rotor models can be combined *a posteriori*, after the respective eigenanalyses have been performed, through a substructuring process. Within TiPa, the technique is based on a generalization of the Craig-Bampton (C-B) approach (ref. [9]). The generation of the wing and rotor substructures is assigned to two independent algorithms. In Fig. 3, the routines are represented by the blocks called WING/ROTOR C-B model generator respectively.

In general, substructuring approaches are based on the identification of the *internal* and *boundary* portion of each submodel, by splitting the model degrees of freedom (DOFs). The Craig-Bampton process applies a partial modal reduction to each substructure leaving their boundary DOFs untouched.

The C-B transformation is defined by the linear map

$$(1) \quad T_{CBR} = \begin{bmatrix} \Phi & \Phi^L \end{bmatrix} \quad \begin{matrix} I & 0 \\ 0 & R \end{matrix}$$

where:

- $\Phi^L$  are the normal modes of each substructure in constrained configuration (fixed boundary DOFs)
- $\Phi^R$ , also called *static shapes*, are the shapes deriving from unit displacements of the boundary degrees of freedom

**Multibody application:** MBDyn performs a direct eigenanalysis on the equations of motion written in DAE form [8]. Therefore, the resulting linearized system of equations is still written with respect to the redundant coordinate set  $q = p \times \lambda^T$ , in descriptor form:

$$(2) \quad \dot{q} = Aq$$

Where  $p$  contains the (dynamic, i.e. having associated inertial properties) nodes momenta,  $x$  the nodes positions and orientations, and  $\lambda$  the Lagrange multipliers associated with algebraic constraints.

The  $A$  and  $E$  matrices associated to the submodels can be used to easily identify  $\Phi^L$ , but not  $\Phi^R$ . This happens since the use of a formulation equivalent to the FEM one to generate the  $\Phi^R$  would require inverting matrix  $A$ , which can be structurally singular. Instead, the static shapes constituting the columns of  $\Phi^R$ , are generated independently from current analysis. To correctly generate such shapes, two considerations need to be made. Firstly, despite the  $q$  vector structure, only the nodal DOFs  $x$  must be properly tuned generate the correct  $\Phi^R$  matrix. This is true since the static shapes are defined in an equilibrium condition, hence the contribution provided by the  $\lambda$  components is null since they define internal forces. Secondly, each MBDyn node has twelve DOFs (3 positions, 3 orientation parameters, 3 momenta and 3 momenta moments). So, since the number of static shapes is associated to the numbers of the boundary nodes DOFs, twelve shapes are needed. This is twice the number of those needed in a conventional FEM approach. This problem was solved by generating the six static shapes associated to unit perturbations of position and rotation DOFs and consequently reusing them by translating to the left momenta DOFs.

The approaches used to define each subsystem shapes are slightly different.

The wing model, it is possible to directly extract the FEM-like matrices describing its beam structure from MBDyn system matrices, that can be in turn used to generate the wing static shapes by performing static analyses corresponding to prescribed displacements and rotations of the wing tip node. These shapes are then redistributed to an MBDyn-like twelve DOFs node structure to complete the generation the wing portion of  $\Phi^R$ .

The definition of the rotor static shapes requires more care. This time, the boundary node is represented by the node clamping the system to the ground. As consequence,

$\Phi$  contains proper rigid body motions, therefore they are generated directly defining the associated nodes' displacements. Once again, the twelve shapes are generated in groups of six,

### 3 DAKOTA AND TIPa

A schematic representation of the DAKOTA/TiPa interaction is

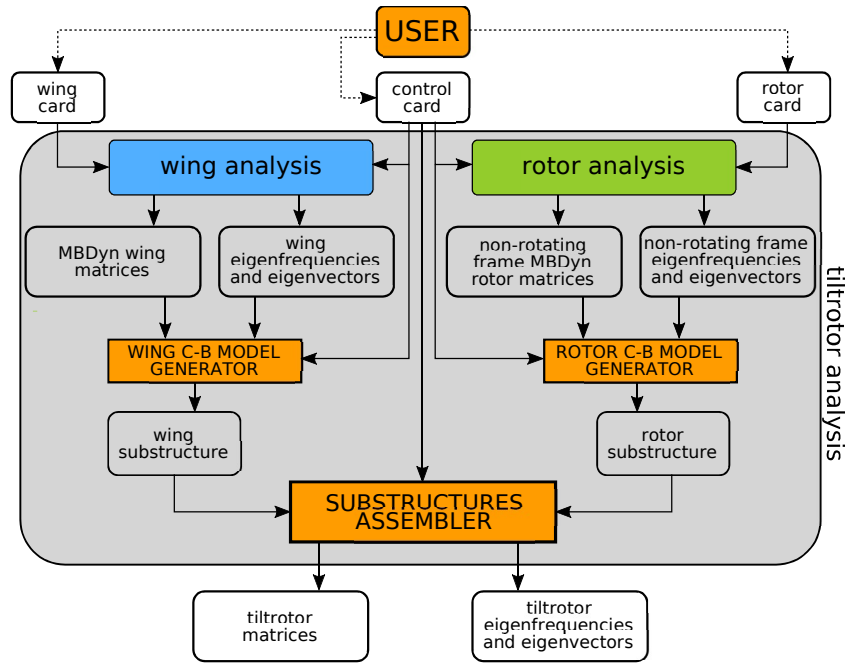


Figure 3: TiPa alternative tiltrotor model generation and analysis.

repeating those generated for position and orientation perturbations to describe the motions associated to the interface momenta DOFs.

Since the rotor behaviour is described in multiblade coordinates, the rotor rigid body motions need to be assessed with such coordinates as well. For this reason, the shapes are generated using the conventional MBDyn DOFs and are eventually transformed to the non-rotating frame coordinates with the MBC transformation matrix  $M$ :

$$(3) \quad \mathbf{q} = (\mathbf{R}_{\text{tot}} \mathbf{P}_{\text{Tmb}}) \mathbf{q}_{\text{mb}} = \mathbf{M} \mathbf{q}_{\text{mb}}$$

where  $\mathbf{q}$  is the MBDyn generalized coordinates vector and  $\mathbf{q}_{\text{mb}}$  is its MBC version. More details on the definition of the MBC transformation matrices can be found in App. A. Thanks to  $M$ , the rotor rigid body motions can be described in the non-rotating frame  $\Phi_{\text{mb}}^R$ :

$$(4) \quad \Phi_{\text{Rmb}} = (\mathbf{M})^{-1} \Phi_R$$

The normal modes contained in  $\Phi^L$ , described with respect to the multiblade coordinates, are directly obtained by the eigenanalysis performed on on the MBC system matrices  $A_{\text{mb}}$  and  $E_{\text{mb}}$ .

The wing and rotor substructures are eventually assembled by the substructures assembler algorithm.

presented in Fig 4. The overall DAKOTA/TiPa assessment, based on the non-intrusive generalized Polynomial Chaos Expansion (gPCE) approach [10, 11], is divided into two phases: the definition of the TiPa analysis surrogate model, and the assessment of the model response stochastic content. The first has the purpose of providing a process representation much simpler to handle with respect to the original one. If the real system response is  $X(\theta)$ , the gPCE formulation provides an approximation  $X_e(\theta)$  as an expansion of polynomial basis  $\Phi^j(\xi(\theta))$  whose definition depends on the probabilistic definition of the input random variables  $\xi(\theta)$ . The deterministic coefficients  $c^j$  are used to tune the representation:

$$(5) \quad X_e(\theta) = \sum_{j=0}^s c^j \Phi^j(\xi(\theta)) \approx X(\theta)$$

The detailed theoretical frame behind this formulation is beyond the scope of this paper. The interested reader is referred to the cited bibliography, and to the DAKOTA documentation.

DAKOTA, as a first step, generates the polynomial basis  $j(\xi(\theta))$ .

The task, that can be regulated through DAKOTA

$\Phi$

input file, is completed by a gPCE basis generator algorithm according to the user provided information about the nature of the process random input(s)  $\xi(\theta)$ . The coefficients  $c^j$  are consequently tuned by DAKOTA with the iterative execution of TiPa. The process, that happens entirely inside a DAKOTA run, can be easily visualized in Fig. 4. The DAKOTA random input variable generator algorithm evinces a deterministic value of  $\xi(\theta)$  according to the user defined input probabilistic distribution. The parameter is consequently provided to TiPa,

which stores the received variable either in the wing or rotor card. The tiltrotor analysis block contains one between the two processes presented in Fig. 2 and Fig. 3. Since  $\xi(\theta)$  affects the tiltrotor geometry or properties definition, each time such variable is provided to TiPa, the complete generation of a new model is required.

Once TiPa analysis is complete, the second interaction occurs. From the tiltrotor simulation some output variables are provided back to DAKOTA. These parameters represent the  $j$ -th loop responses and are collected by a random output variable collector algorithm. The responses the user wants DAKOTA to collect are defined through the software input file (see ref. [7]). In this application, they usually store information about the whirl flutter critical modes frequency estimates and damping factors. In case multiple response variables are considered, different response functions  $X_e(\theta)$  are computed.

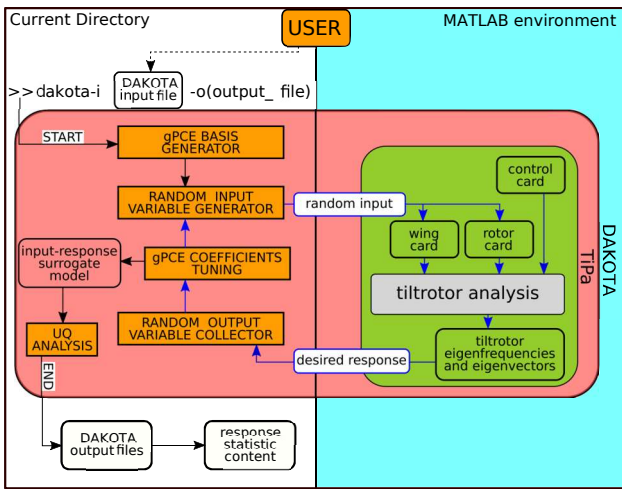


Figure 4: Scheme of a DAKOTA/TiPa interaction.

The  $j$ -th output variables are provided to a gPCE coefficients tuning scheme in order to identify the values of the expansion coefficients  $c^i$ . The process, started with the random input variable generation, is repeated iteratively according to DAKOTA internal design as long as all the coefficients are computed. This loop is presented in Fig. 4 with blue arrows.

Once the tuning is complete, the cycle ends and the surrogate model is entirely defined. This new model is used to compute the system output stochastic behaviour since it represents the relationship between the random input parameters  $\xi(\theta)$  and an approximation of the random response  $X_e(\theta)$  through a polynomial representation. The approximated definition is very convenient because, on one side, the expansion coefficients  $c^i$  already provide statistic information about the real uncertain response  $X(\theta)$  while, on the other, the new polynomial description allows the computationally inexpensive application of Monte Carlo-like sampling methods to assess the output probability and cumulative distribution functions as well as the input-output sensitivity indices. This process is represented in Fig. 4 in the block called UQ analysis.

After this operation, the assessment is complete. DAKOTA saves the results in a series of output text files and stops its run. It is important to point out that during the entire process DAKOTA is not aware about the internal structure of TiPa. The two interactions happening through the interface between the two software are the only elements necessary to complete the assessment. This is the strong feature of the *non-intrusive* gPCE formulation.

The process explained in the previous section shows a non-negligible problem. During an UQ assessment, TiPa input cards are only accessible by DAKOTA. For this reason, as already mentioned, the user must tune the model design and simulation properties (excluding the random variables provided by DAKOTA) before the UQ software is executed. The problem lies in the fact that the information about the wind tunnel air properties (speed, density,...) are stored in the control card.

Therefore, the whole process is controlled by a UNIX shell script, referred to as DAKOTA TiPa.sh in Fig. 5: the  $N$  desired airspeed values to test the aeroelastic model with are defined in the first part of the script. The tiltrotor model is still not accessible during the simulation: therefore, the model features must be tuned before the assessment starts.

The DAKOTA/TiPa analysis executed in this process is the same one presented in section 3 and in Fig. 4 in the block with the reddish colour. Only one detail is different. TiPa, before starting its analysis, imports the  $i$ -th simulation airspeed data. The process can be easily visualized on the right side of the DAKOTA/TiPa block in Fig. 5. This allows the automatic update of MBDyn simulations airspeed values during external loop progress. Within the  $i$ -th loop, the flight speed remains constant. Once the DAKOTA/TiPa analysis is complete, the responses stochastic data are stored in the  $i$ -th output files.

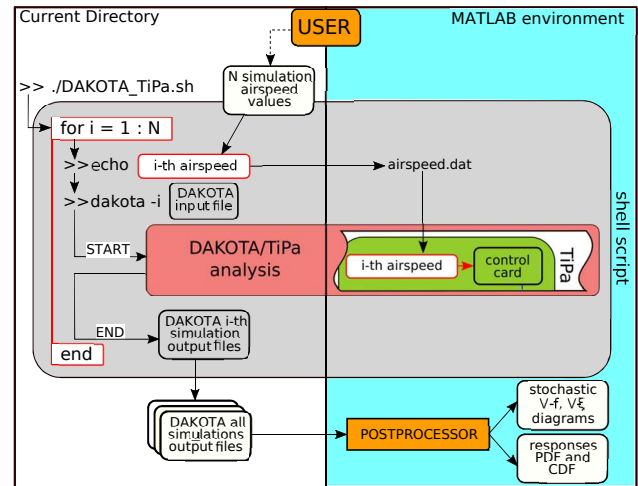


Figure 5: Scheme of a complete DAKOTA/TiPa aeroelastic assessment.

The entire collection of DAKOTA simulations output files is eventually parsed by a MATLAB postprocessor which imports the interesting results in the numerical environment.

The typical response variables analyzed are the frequencies ( $f$ ) and the damping ( $\xi$ ) associated to the system modes that may lead to the whirl flutter phenomenon development. In such cases, plotting the  $i$ -th loop DAKOTA responses characterizations over the  $i$ -th airspeed values provides a stochastic visualization

of the  $V-f$  and  $V-\xi$  diagrams. DAKOTA also outputs the responses' Probability Density Functions (PDF), the Cumulative Distribution Functions (CDF) and the Sobol indices estimates, providing information about how each input parameter affects a given response function.

## 4 APPLICATIONS

Two examples of DAKOTA/TiPa analyses are shown in the first part this section. The assessments have been performed on a simplification of the three bladed stiff in-plane version of the WRATS model, generated entirely with TiPa. Please note that such model represents a simpler version of the original WRATS test-bed. In this part, the tested tiltrotor is generated entirely in MBDyn through the conventional modelling approach.

In the second part, instead, some insight about the alternative modeling approach described in Section 2.2) is presented. Despite the method showing some interesting and encouraging early results, its validation, at this stage of the development, is not complete yet. The state of the art, and the steps that led to the validation of most of the entire procedure, are presented along with the description of the path to complete the assessment of the process in future research campaigns.

### 4.1 The WRATS model

The tiltrotor model used as reference is the three bladed stiff in-plane version of the WRATS test-bed model (Cf. Fig. 6) [12, 6].

To obtain the most consistent analysis conditions, the entire range of simulations was executed with the rotor in *windmill* condition: the zero torque trim case.



Figure 6: Tiltrotor multibody model in MBDyn.

The tests were entirely executed with the rotor angular speed set to 742 RPM which, according to the data used, represents the reference angular speed in airplane mode for the WRATS test-bed.

### 4.2 UQ parameters tuning

The gPCE method relies on the definition of a surrogate model to execute the Uncertainty Quantification assessments. For this reason, the accuracy of the analysis results strongly depend on the quality of the defined approximated model. Its precision is regulated by the order of the polynomial approximation used to generate it. For this reason, some investigations were executed to identify the optimal number of polynomial coefficients to use in the definition of each iteration surrogate response models.

To do so, a series of analysis were run to understand the stochastic variation of the WRATS isolated wing model first bending mode frequency under an uncertain mass distribution. This random parameter was chosen since it would have extensively affected the system response value. The tests were executed increasing the order of the Gaussian quadrature rule used to compute the multidimensional integration necessary evaluate the gPCE coefficient values. The number of evaluated gPCE coefficients matches, in this simple case, the quadrature order.

PCE coeff.	Mean value	Variance	Time [s]
1	19.694080	0.0	25
2	19.712230	0.488563	55
3	19.712295	0.490745	77
4	19.712296	0.490765	103
5	19.712306	0.490784	143

Table 1: Effects of gPCE order on reference analysis results.

Table 1 shows how the gPCE order mostly affects the variance esteem of the random response rather than its mean value. Despite this, the average and variance evaluations converge rapidly as the polynomial order is increased.

It is now important to point out that DAKOTA does not rely on the gPCE coefficients values to compute the local and global sensitivity indices during each analysis. They are evaluated from the sampling methods assessments executed on the surrogate model. For this reason, no extra gPCE coefficients are required to obtain quality sensitivity indices.

So, for the entire sets of analysis presented in the following sections, a fourth order polynomial expansion has been used during the assessments. This was considered to be an optimal solution both in terms of accuracy and in terms of efficiency since, in the following analysis, a limited number of random input and response variables was considered. In case a larger set of parameters are investigated, the use of a lower order polynomial expansion is suggested to maintain a reasonable execution time.

### 4.3 DAKOTA/TiPa analysis results

This section presents some examples of DAKOTA/TiPa analysis results. The assessments were performed using the *conventional* TiPa tiltrotor whirl flutter modelling approach, i.e. the parametric generation of the entire assembly within a single MBDyn model.

### 4.3.1 Single random input parameter propagation

In this example, an uncertain distribution of the wing bending stiffness about the model  $Y$ -axis (aligned with the incoming wind speed direction) is assumed. The investigation aims at evaluating the system response statistical distribution when the bending stiffness properties are extracted from a cluster of values close to the nominal ones: the reference wing out of plane bending stiffness  $EJ_y$  is pre-multiplied by a normal distribution  $N(\mu, \sigma^2)$  with mean value  $\mu = 1$  and standard deviation  $\sigma = 0.05$ .

**Stochastic  $V$ - $f$  and  $V$ - $\xi$  diagrams:** the first outcomes of the analysis are the stochastic  $V$ - $\xi$  and  $V$ - $f$  diagrams (Fig. 7). They provide a visual representation of how the system random responses (the beam mode frequencies and damping) are assessed assuming uncertain input variables. The collection and investigation of the first bending mode properties as response variables is due to the fact that, in the original WRATS model, it is possible to investigate the aeroelastic stability of the system through the definition of this mode stability margin.

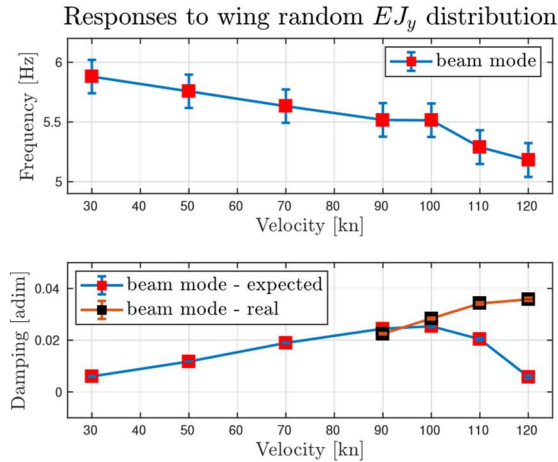


Figure 7: Single input stochastic  $V$ - $\xi$  and  $V$ - $f$  diagrams.

In both plots, the red squares are placed at the responses mean values computed at each airspeed condition, while the standard deviation is visualized through the error bars.

In Fig. 7 two different damping trend are presented for speeds higher than 90 kn. The blue line represents the expected trend, as found in previously validated work on the modeling of the WRATS (Ref. [13]). The orange and black one, instead, represents the stability margin derived from its simplification used in the assessments. The real data is not presented for airspeeds lower than 90 kn since the two trends are almost identical. The representation of both curves, though, has the purpose of underlying the fact that the analysis presented in this section do not try to get any specific conclusion about the WRATS model design. They are simply presented to show the possible outcomes of the stochastic prediction tool.

In this example, it is clear that the random input parameter is mostly affecting the beam mode eigenfrequency while leaving almost untouched the mode damping quantification. The latter actually shows an increasing trend in the variability of the

response as the airspeed is increasing. To further highlight this aspect, sensitivity indices can be evaluated.

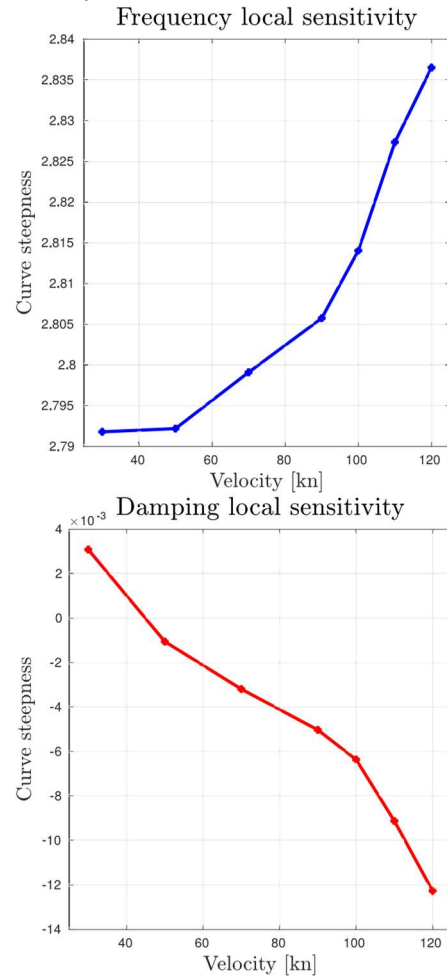


Figure 8: Responses local sensitivity to random  $EJ_y$ .

**Local sensitivity:** by definition [14], this parameter is the slope of the system response to input variation, evaluated through two couples of parameters: a reference input value and its associated system response, and a second input value computed as an increment of the reference one, with the related system response. Figure 8 shows the responses local sensitivity indices to the random wing  $EJ_y$  distribution. It is evident that there is an increase in the sensitivity of the beam mode eigenfrequency to the random input value as the airspeed increases, indicating that as the incoming wind speed rises, if the same perturbation in the system input is introduced, the evinced eigenfrequency value derived from the perturbed input tends to increase. The damping associated local sensitivity indices have a magnitude significantly lower than the frequency ones. The interesting feature of the damping local sensitivity trend, though, is represented by the change of sign of such sensitivity indices as the airspeed increases. This means that for the same positive increase of the input variable, the beam mode damping value is either increased (at about 30 kn) or decreased (at all the other tested speeds). This provides a very useful insight about the *direction* of the system response at different speeds.

**The responses PDF and CDF curves:** another feature provided by a DAKOTA/TiPa analysis is the assessment and identification of the responses stochastic curves. An example of such outputs is presented in Fig. 9 which shows the PDF and CDF curves representing the stochastic characterization of the beam mode eigenfrequency at 30 kn. The PDF curve representation is superimposed with the response mean value (dashed line) and its standard deviation (two diamonds). The response associated PDF curve maintains the input normal distribution shape with associated skeweness  $\mu_3 \approx 0$  and kurtosis  $\mu_4 \approx -2$ .

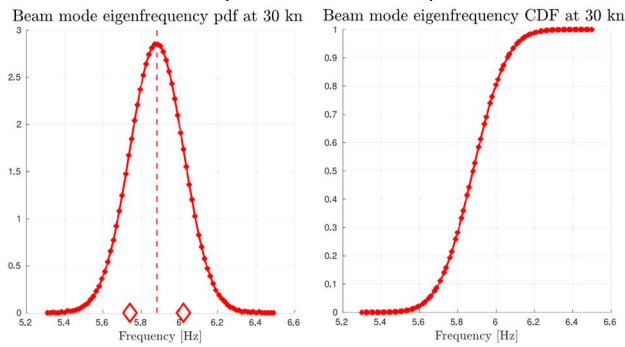


Figure 9: Beam mode frequency PDF and CDF curves with random wing  $EJ_y$ .

**Analysis time:** Table 2 shows a detail of the execution times of the package different modules.

TiPa [s]	DAKOTA [s]	Total [s]
3311	20	3331

Table 2: Single random input propagation simulation times.

**DAKOTA execution** refers to the actual time spent by the software generating the polynomial basis, tuning the expansion coefficients and executing the UQ analysis. This is pointed out since, as explained in section 3, most of the entire process actually happens inside DAKOTA environment.

For each investigated speed, a surrogate model of the random input/output relationship is developed. A single complete TiPa/MBDyn tiltrotor assessment requires about 120 s. For this reason, with the used fourth order approximation, four successive runs need to be executed to complete the approximated system representation. Once each surrogate model is ready, DAKOTA, draws 10000 samples from the stochastic input definition and executes a LHS (Latin Hypercube Sampling) UQ assessment on the polynomial representation of the system. This allows the evaluation of the response PDF, CDF and the sensitivity indices of the analysis. This final assessment is extremely fast.

Of course the responses stochastic content is, in turn, not evaluated using the complete model but by means of an approximation of it. This can potentially affect the results reliability, and highlights the importance of the selection of the proper polynomial expansion order.

### 4.3.2 Two random input parameters propagation

In order to provide a reasonable comparison with the assessment presented in section 4.3.1, the wing beam  $EJ_y$  stiffness randomness is used in this investigation as well. The parameter maintains the same stochastic definition of the previous analysis. As new non-deterministic parameter, a random definition of the pylon mass value  $M_p$  is introduced in the formulation. The parameter stochastic distribution has been assumed to be well-described by a uniform distribution defined in the  $\pm 20\%$  range centered about the nominal value. No particular physical meaning has to be assigned to the choice of such distribution: it has been selected to provide an example of the possibility to execute analysis with different shapes of the input variables PDF curves.

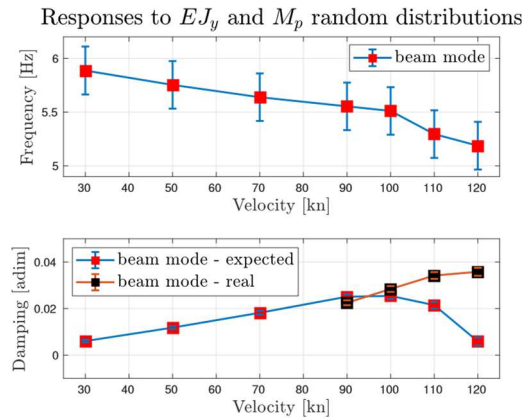


Figure 10: Two inputs stochastic  $V-\xi$  and  $V-f$  diagrams.

**Stochastic  $V-f$  and  $V-\xi$  diagrams:** The stochastic  $V-f$  and  $V-\xi$  associated to this assessment are presented in Fig. 10. Please note that the same concepts discussed in the description of Fig. 7 beam mode damping trend are valid here. The model used in the analysis does not try to exactly emulate the WRATS behaviour, but it is meant to show the possible outcomes of some reference DAKOTA/TiPa analysis. The curves shows a similar trend compared to those presented in Fig. 7. When the second random variable is introduced, though, the responses standard deviation tends to increase with respect to the case in which only one appears. It is interesting to notice how, in this second analysis, the beam mode damping standard deviation increment as the airspeed rises is more evident compared to the previous case.



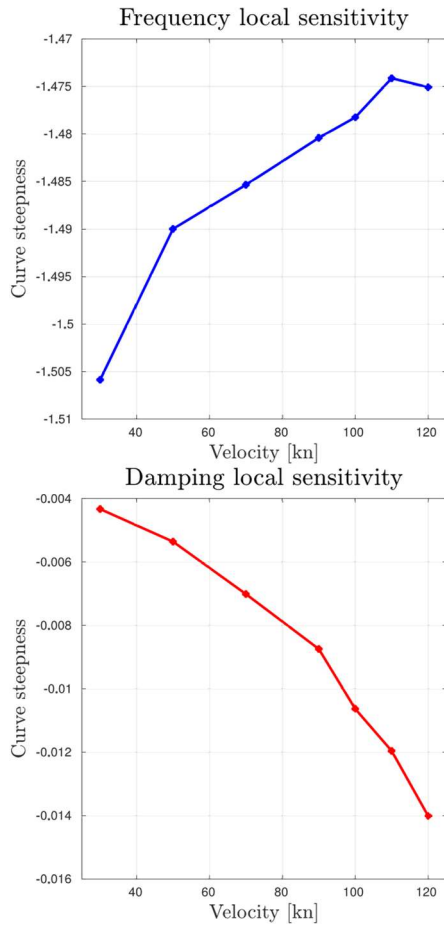


Figure 11: Responses local sensitivity to random  $M_p$ .

**Local sensitivity:** Figure 11 shows the local sensitivity indices of the system responses to the variability in the  $M_p$  value. The represented trends shows that both responses tend to decrease in response to an increment in the mass value since the local sensitivity indices always have a negative value. This trend is maintained through all the tested airspeeds. The comparison between the damping local sensitivity indices represented in Fig. 8 and Fig. 11 shows that this parameter is more influenced by an increment in the  $M_p$  with respect to a variation of the  $EJ_y$  definition, since the sensitivity indices to the mass pylon value are one order of magnitude larger with respect to those related to the bending stiffness.

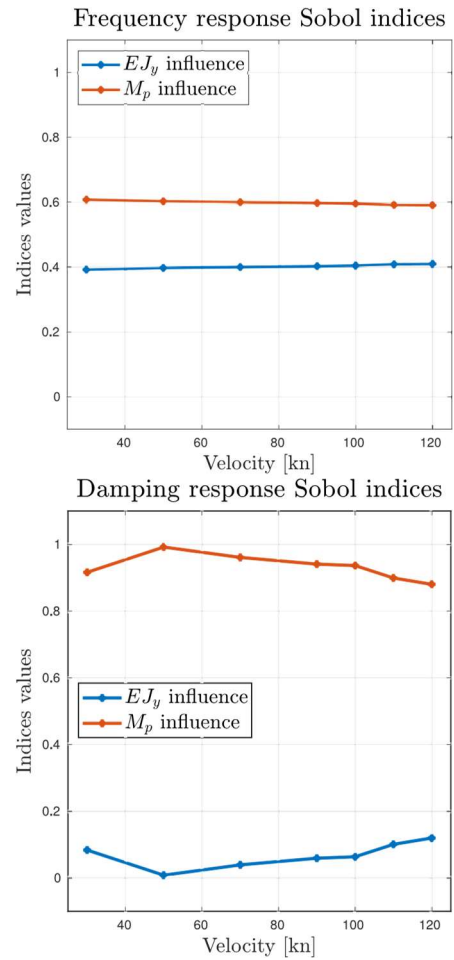


Figure 12: Sobol indices associated to the system responses.

**Global sensitivity:** When multiple random input parameters are defined, the DAKOTA/TiPa package can also be used to compute Sobol indices. They are used to execute global sensitivity analysis, since they provide a quantification of each random input variable contribution to the responses variance (ref [14, 15]). This gives a deep insight about the actual role of each non-deterministic parameter in the system overall behaviour. Each Sobol index value is between 0 and 1 and the sum of all the indices associated to a given analysis is always unitary.

In Fig. 12, the values of the Sobol indices indicating the influence of each random parameter input on the variance of the beam mode eigenfrequency and damping at the tested airspeeds is shown. Please note that a third index is always estimated when two random variables are introduced in a system. This is meant to assess the contribution of the *interaction* between the two variables to the responses variance. In the presented analysis, as can be expected, very little interaction appears in the results and for this reason it is not reported.

Sobol indices provide very useful insight on the influence each parameter has on the analyzed system response. During an aeroelastic analysis, the main purpose usually will be on which parameters affect the stability margin the most. From Fig. 12, it is clear that randomness of the pylon mass has a larger influence on the beam mode damping variability with respect to the wing stiffness. This, in this simple test, may be due to the two different and arbitrary definitions provided to the input variables

stochastic definitions. In a more realistic case, though, when two (or more) comparable sources of randomness are introduced in the model, the information provided by the Sobol indices can be very powerful and intuitive.

**The responses PDF and CDF curves:** Figure 13 shows the PDF and CDF distributions of the beam mode eigenfrequency evaluated at 30 kn. By comparison with Fig. 9 PDF distribution, it is possible to identify how the new parameter affects the system stochastic response in the same tested airspeed condition.

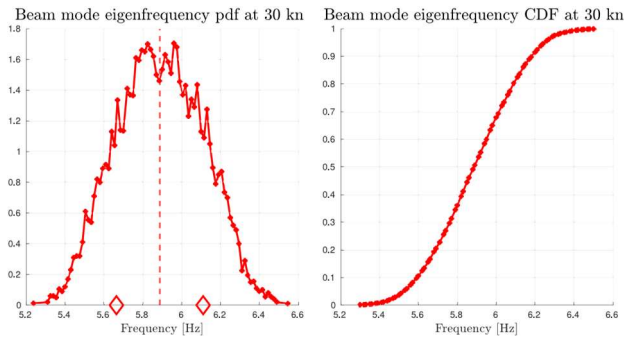


Figure 13: Beam mode frequency PDF and CDF curves with random wing  $EJ_y$  and  $M_p$ .

The change in the PDF properties can be assessed as well in through its shape defining parameters: the skewness  $\mu_3^{\sim} = 0.04195$  and the kurtosis  $\mu_4^{\sim} = -1.0461$

**Analysis time:** the DAKOTA/TiPa execution time is, in this analysis, extensively affected by the presence of the second random input variable. Table 3 shows the details about the simulation times.

TiPa [s]	DAKOTA [s]	Total [s]
8522	52	8574 sec

Table 3: Two random inputs propagation simulation times.

The analysis time is increased by both the fact that a larger number of TiPa executions is required (in order to tune the gPCE coefficients) and by the increased number of random input variables.

#### 4.4 The substructuring approach

This section is designed to present the early results obtained with the substructuring approach. The procedure, at the time of writing, is still under development and only partial results are available. The state of the art of the procedure is here presented, alongside the outline of the future developments.

##### 4.4.1 Reference set-up

In order to develop a consistent representation of the whirl flutter phenomenon, during each component substructuring process a precise set of constrained normal modes  $\Phi^L$  has been

used in the construction of the Craig-Bampton matrices of each subsystem. The selected mode shapes used in the definition of the wing and rotor substructuring matrices are listed in Tab. 4.

Wing normal modes	Rotor normal modes
1st bending OoP (Beam)	Gimbal
1st bending InP	Cone
2nd bending OoP	1st collective/cyclic Beam
2nd bending InP	1st collective/cyclic Lead-Lag
1st torsion	...

Table 4: Normal modes used in substructuring matrices.

Where *OoP* means *Out of Plane* while *InP* means *In Plane*. The . . . are placed in Tab. 4 right column to point out that while the normal modes types and numbers used in the wing substructuring process has been maintained as constant during the whole process, since they are expected to be sufficient to model the motion cause by whirl flutter, the use of different shapes associated to the rotor subsystem have been investigated.

**The rotor substructure:** The rotor substructure describes a free-free element since only a single node is connected to the ground in the original constrained model. These degrees of freedom are *freed* by the introduced rigid body motion shapes necessary to generate the system associated C-B matrix. In order to verify the effectiveness of the used rigid body motion shapes, an equivalent model has been generated.

To test the validity of the transformation, we first compared the MBDyn original clamped rotor with its free-free corresponding substructured model with a very large pylon mass ( $M_p$ ) attached to its interface node to *reintroduce* the clamp and make the two systems comparable. This is meant to investigate the effectiveness of the introduced rigid body motions and possible modifications of the structural normal modes. Table 5 shows comparison between the two system normal modes nondimensional eigenfrequencies in column two and three. The model were tested in vacuo at 742 RPM, the regime condition. Please note that both systems are described in multiblade coordinates.

Table 5 shows a clear matching in the two system representations. This proves that the rigid body shapes generated and introduced in the system through the CB matrix do not alter the rotor flexible behavior.

Mode name	MBDyn model [1/rev]	Subst. w large $M_p$ [1/rev]	MBDyn rotating [1/rev]
Gimbal	$\approx 0$	$\approx 0$	1
	1.98	1.99	1
Cone	1.18	1.18	1.18
1st coll L-L	1.63	1.63	1.63
1st cyc L-L	0.62	0.61	1.62
	2.62	2.61	1.62

Table 5: Clamped MBDyn and substructured rotor modes comparison.

With the exact value of the pylon mass, the rotor substructured model eigenfrequencies slightly changes with respect to the clamped system ones. The modes shapes, as well, adapt to the free interface condition. As example of this, in Fig. 14, the coning mode of the rotor substructure is presented. There, it is easy to identify the displacement of the mast and hub nodes with respect their initial position. This matches the expected behavior of the system with free interface. Among the eigenmodes associated to this substructured system some pure rigid body motions appear as well.

Beam mode shape

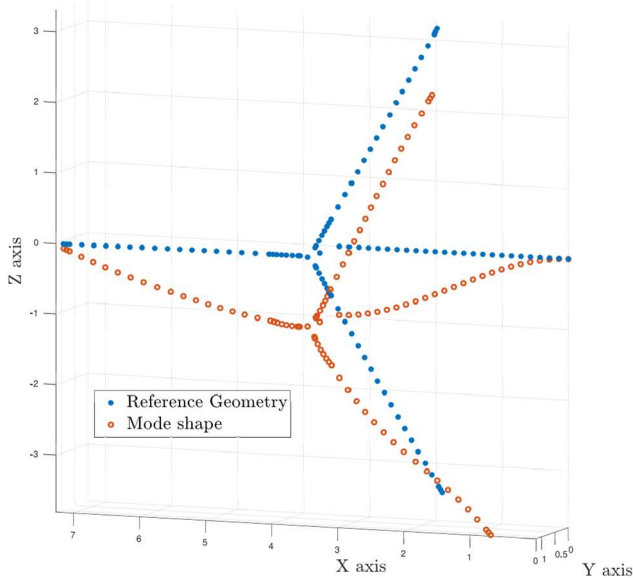


Figure 15: Beam mode shape from tiltrotor substructured model.

The thorough validation of the substructuring procedure with a complete free-free rotor model is left to future investigation.

**The full tiltrotor model** The alternative approach proved to be effective in the reconstruction of the proper tiltrotor system mode shapes since they appear to be very similar to those associated to the entire MBDyn tiltrotor model. In Fig. 15, for instance, the beam mode shape of the tiltrotor generated with the C-B approach is represented. The shape was reconstructed starting from the eigenvectors associated to the substructured system matrices. However, more work is still to be done on the complete validation of the substructuring approach, as the complete aeroelastic behavior of the full tiltrotor system is still not matched with a sufficient level of confidence at the time of writing.

## 5 CONCLUSIONS

The development of a stochastic parametric tiltrotor whirl flutter prediction tool is presented. The tool is based on the interaction of three elements: a parametric tiltrotor model generator called TiPa, the multibody generalpurpose aeroelastic solver MBDyn and the state of the art Uncertainty Quantification software DAKOTA. The interaction of the three has been designed to provide an effective investigation tool to support the current research in the field. TiPa has been developed specifically to provide a flexible interface to the modelling of an arbitrary configuration tiltrotor assembly.

The parametric conception of TiPa proved to be an essential feature to introduce a forward propagating Uncertainty Quantification (UQ) method in the formulation, based on the non-intrusive generalized Polynomial Chaos Expansions (gPCE) technique, implemented in DAKOTA. Thanks to the introduction of the UQ techniques, it is possible to execute complete sensitivity analysis of the desired input parameters effects. Moreover, the system non-deterministic response to such variables is estimated through the definition of the stochastic  $V-f$  and  $V-\xi$  diagrams and the outputs PDF and CDF curves.

TiPa provides two different modelling approaches to define the complete tiltrotor assembly. The first option is based on the definition of an entire wing/proprotor MBDyn model, while the other relies on the generation of two individual subsystems to be joined through a substructuring approach. The second method is aimed at providing a consistent representation of the rotor dynamics through an original adaptation of the multiblade coordinates (MBC) transformation, applied directly to the redundant coordinates of the multibody system, and an original application of the CraigBampton substructuring approach.

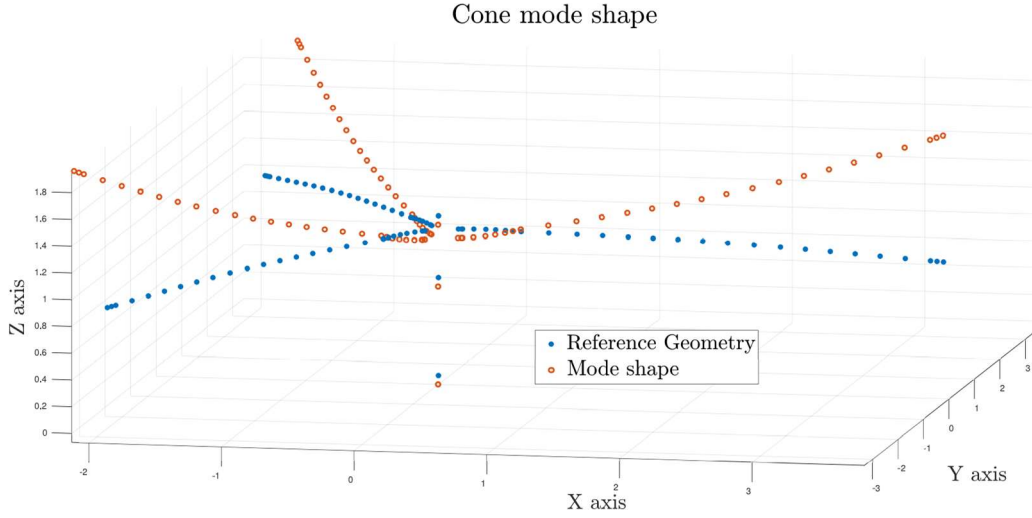


Figure 14: Coning mode of the rotor substructure.

## Acknowledgments

The research leading to these results has received funding from the Clean Sky 2 – H2020 Framework Programme, under the grant agreement N.863418, (the ATTILA project).

## Copyright Statement

The authors confirm that they, and/or their company or organization, hold copyright on all of the original material included in this paper. The authors also confirm that they have obtained permission, from the copyright holder of any third party material included in this paper, to publish it as part of their paper. The authors confirm that they give permission, or have obtained permission from the copyright holder of this paper, for the publication and distribution of this paper as part of the ERF proceedings or as individual offprints from the proceedings and for inclusion in a freely accessible web-based repository.

## A Multiblade coordinate transformation for multibody systems

Assuming that the  $k$ -th blade motion is described by a single and generic degree of freedom  $q^k$ , that DOF can be rewritten as a linear combination of the system multiblade coordinates [16, 17] in the following form:

$$(6) \quad q^k = q_0 + \sum_n (q_{nc} \cos n\psi_k + q_{ns} \sin n\psi_k) + q_{Nb/2} (-1)^k$$

where an  $N_b$  blade rotor is assumed the blade azimuth angle  $\psi_k$  is

$$(7) \quad \psi_k = \psi + (k-1) \frac{2\pi}{N_b}$$

The change of coordinates is represented by the matrix  $T(\psi)$ :

$$(8) \quad \mathbf{q} = T(\psi) \mathbf{q}_{mb}$$

The entire multibody system structural coordinates defined with respect to MBDyn global reference frame  $x$  can be grouped as:

$$(9) \quad \mathbf{x} = \begin{Bmatrix} \mathbf{x}^0 \\ \mathbf{x}_{bl}^1 \\ \vdots \\ \mathbf{x}_{bl}^n \end{Bmatrix}$$

where  $\mathbf{x}^0$  contains the *non-recursive* dofs, i.e. those not associated with the blades. The latter must be transformed in the local frame of each blade:

$$(10) \quad \begin{Bmatrix} \mathbf{x} \\ \vdots \\ \mathbf{x}_{bl}^n \end{Bmatrix} = \begin{bmatrix} R_{bl}(\psi_1) & & \\ & \ddots & \\ & & R_{bl}(\psi_n) \end{bmatrix} \begin{Bmatrix} \mathbf{x}^0 \\ \mathbf{x}_{bl}^1 \\ \vdots \\ \mathbf{x}_{bl}^n \end{Bmatrix}$$

where  $\mathbf{x}_{bl}^k$  and  $\mathbf{e}_{bl}^k$  are vectors storing all DOFs related to the  $k$ -th blade defined with respect to global and local reference frames. Matrices  $R_{bl}(\psi_k)$  are block-diagonal, with 3x3 rotation matrices on the main diagonal

$$(11) \quad R_z^k = \begin{bmatrix} \cos(\psi_k) & -\sin(\psi_k) & 0 \\ \sin(\psi_k) & \cos(\psi_k) & 0 \\ 0 & 0 & 1 \end{bmatrix}$$

The formulation can be compressed in:

$$(12) \quad \mathbf{x} = R^x(\psi) \mathbf{x}_e$$

Similar considerations apply to Lagrange multipliers associated with blade joints:

$$(13) \quad \boldsymbol{\lambda} = R^\lambda(\psi) \tilde{\boldsymbol{\lambda}}$$

The MBDyn state vector  $\mathbf{q}$  is described with respect to local blades reference frame through:

$$\begin{aligned} \left\{ \mathbf{x} \right\} &= \begin{bmatrix} \mathbf{R}^{\mathbf{x}}(\psi) & \mathbf{0} \\ \mathbf{0} & \mathbf{R} \end{bmatrix} \begin{Bmatrix} \tilde{\mathbf{x}} \\ \tilde{\lambda} \end{Bmatrix} \quad (14) \quad \mathbf{q} \\ &= \mathbf{R}_{\text{tot}}(\psi) \mathbf{q}_e \end{aligned}$$

The overall transformation is given by

$$(15) \quad \mathbf{q} = (\mathbf{R}_{\text{tot}} \mathbf{P} \mathbf{T}_{\text{mb}}) \mathbf{q}_{\text{mb}} = \mathbf{T} \mathbf{q}_{\text{mb}}$$

where  $\mathbf{P}$  is a permutation matrix used to reorder the degrees of freedom in the shape  $\mathbf{q} = \{\mathbf{p}\mathbf{x}\lambda\}^T$ .

## REFERENCES

- [1] ACARE — Report of the Group of Personalities. European aeronautics: a vision for 2020, January 2001.
- [2] Eric Hathaway and Farhan Gandhi. Tiltrotor whirl flutter alleviation using actively controlled wing flaperons. *AIAA Journal*, 44(11):2524–2534, 2006. doi:10.2514/1.18428.
- [3] M. Mataboni, P. Masarati, G. Quaranta, and P. Mantegazza. Multibody simulation of integrated tiltrotor flight mechanics, aeroelasticity and control. *J. of Guidance, Control, and Dynamics*, 35(5):1391–1405, September/October 2012. doi:10.2514/1.57309.
- [4] Jiří Čerňák. Whirl flutter-related certification according to far/cs 23 and 25 regulation standards.
- [5] Wilmer H Reed. *Review of propeller-rotor whirl flutter*. National Aeronautics and Space Administration, 1967.
- [6] Pierangelo Masarati, David J Piatak, Giuseppe Quaranta, Jeffrey D Singleton, and Jinwei Shen. Soft-inplane tiltrotor aeromechanics investigation using two comprehensive multibody solvers. *Journal of the American Helicopter Society*, 53(2):179–192, 2008.
- [7] Brian M Adams, WJ Bohnhoff, KR Dalbey, JP Eddy, MS Eldred, DM Gay, K Haskell, Patricia D Hough, and Laura P Swiler. Dakota, a multilevel parallel object-oriented framework for design optimization, parameter estimation, uncertainty quantification, and sensitivity analysis: version 5.0 user’s manual. *Sandia National Laboratories, Tech. Rep. SAND2010-2183*, 2009.
- [8] P. Masarati. Direct eigenanalysis of constrained system dynamics. *Proc. IMechE Part K: J. Multi-body Dynamics*, 223(4):335–342, 2009. doi:10.1243/14644193JMBD211.
- [9] Roy R. Craig, Jr. and Mervyn C. C. Bampton. Coupling of substructures for dynamic analysis. *AIAA Journal*, 6(7):1313–1319, July 1968.
- [10] Dongbin Xiu and George Em Karniadakis. The wiener–askey polynomial chaos for stochastic differential equations. *SIAM journal on scientific computing*, 24(2):619–644, 2002.
- [11] Shuxing Yang, Fenfen Xiong, and Fenggang Wang. Polynomial chaos expansion for probabilistic uncertainty propagation. *Uncertainty Quantification and Model Calibration*, page 13, 2017.
- [12] David J Piatak, Raymond G Kvaternik, Mark W Nixon, Chester W Langston, Jeffrey D Singleton, Richard L Bennett, and Ross K Brown. A wind-tunnel parametric investigation of tiltrotor whirl-flutter stability boundaries. 2001.
- [13] J. Shen, P. Masarati, D. J. Piatak, M. W. Nixon, J. D. Singleton, and B. Roget. Modeling a stiff-inplane tiltrotor using two multibody analyses: a validation study. In *American Helicopter Society 64th Annual Forum*, Montreal, Canada, April 29–May 1 2008.
- [14] Jerôme Morio. Global and local sensitivity analysis methods for a physical system. *European journal of physics*, 32(6):1577, 2011.
- [15] Ilya M Sobol. Global sensitivity indices for nonlinear mathematical models and their monte carlo estimates. *Mathematics and computers in simulation*, 55(1-3):271–280, 2001.
- [16] Robert P. Coleman. Theory of self-excited mechanical oscillations of hinged rotor blades. ARR 3G29, NACA, July 1943.
- [17] KH Hohenemser and SK Yin. On the use of first order rotor dynamics in multiblade coordinates. In *30th Annual National Forum of the American Helicopter Society, Preprint No. 831*, 1974.